J. Biochem. **139**, 431–438 (2006)
doi:10.1093/jb/mvj045

Evaluation of the Dynamic Structure of DsrA RNA from *E. coli* and Its Functional Consequences

Katarzyna Rolle*, Marek Zywicki*, Eliza Wyszko, Miroslawa Z. Barciszewska and Jan Barciszewski†

Institute of Bioorganic Chemistry, Polish Academy of Sciences, Noskowskiego 12/14, 61-704 Poznan, Poland

Received October 7, 2005; accepted December 20, 2005

DsrA RNA is an 87-nucleotide regulatory non-protein-coding RNA of *Escherichia coli* for which two secondary structure models (I and II) have been proposed. We have compared these models by the energy calculations, which revealed that the currently accepted model II should be rejected on the basis of thermodynamics. Here we provide new results of nuclease footprinting analysis and the application of RNA technologies that have not previously been used for DsrA RNA structural studies, such as hydrolysis with RNase H, DNAzyme, hydroxyl radicals and lead. These approaches together with bioinformatics calculations provided strong arguments for a new model III. This model clearly shows that the long U-rich region between hairpins 1 and 2 is double-stranded. These findings shed new light on DsrA RNA—Hfq interactions.

Key words: DsrA RNA, non-coding RNAs, regulatory RNAs, RpoS, small RNAs.

One of the most spectacular outcomes of genome sequencing projects is that the complete human genome contains less than 2% of protein-coding genes (*1*). The remaining noncoding part of the genome is a huge source of RNA genes. Despite the lack of efficient methods for their identification, several functional non-protein-coding RNAs (noncoding RNAs, npcRNAs, ncRNAs) deriving from intergenic regions, introns (*2*) and pseudogenes have recently been fished out (*3*). Although the non-protein-coding part of the bacterial genome is relatively small (*ca.* 25%), some ncRNAs capable of posttranscriptional gene silencing have been found (*4*). They usually contain a short nucleotide sequence complementary to a target mRNA in the 5′ untranslated region (UTR). Although ncRNA-mRNA base-pairing can sometimes be imperfect, it can affect the accessibility of a ribosome-binding site (RBS) located in the 5′UTR. There is much evidence that the expression of ncRNAs is induced by different stress conditions.

One of the most extensively studied bacterial small ncRNAs is DsrA RNA. It is a key component of cold shock response machinery in *Escherichia coli* which acts by binding two mRNAs. The first one encodes RpoS, an alternative RNA polymerase sigma subunit responsible for global transcription activation, and the second one encodes H-NS—antagonist of RpoS (*5*). The interaction of DsrA RNA in the 5′UTR of RpoS mRNA is very specific and unique. The binding site is localized about 70–80 nt upstream of the start codon, within a stable stem containing an RBS sequence. DsrA RNA through binding the complementary sequence blocking the RBS induces a release of RBS and initiation of RpoS translation. On the other hand, the interaction in the 5′ and 3′ UTRs of H-NS mRNA causes its translational arrest. The final observed effect is an increase of RpoS and decrease of H-NS proteins contents in a cell. Since these two proteins are antagonists in the transcription regulation, a small variation in DsrA concentration causes critical changes of global transcription level.

It is clear that for a mechanism of regulation by antisense RNAs, both sequence and structural features are important. The complementary sequences in hairpin loops are crucial for an increased rate of complex association and propagation (*6*). Two secondary structures of DsrA RNA have been proposed (*5*, *7*–*9*). They consist of three hairpins. The stem-loops 1 and 3 in both models are identical, but the difference lies in the location and structure of the second hairpin, containing H-NS mRNA–binding site. Part of the region of DsrA RNA binds the ubiquitous and nonspecific RNA binding protein Hfq, which is crucial for interaction with RpoS mRNA (*10*–*12*). Hfq probably acts as an RNA chaperone for DsrA RNA. A decrease of Hfq protein level is associated with extremely fast DsrA RNA degradation. Therefore, Hfq is a key factor in the modulation of DsrA RNA activity and it affects the RpoS translation.

Up to now, DsrA RNA has only been found in *Escherichia coli*, *Salmonella typhimurium*, *Salmonella enterica* and *Klebsiella pneumoniae* out of more than 220 sequenced bacterial genomes. Since another two components of the above-described regulatory system, RpoS and Hfq, have been identified for a variety of species, it is reasonable to expect the same for DsrA RNA. Recently, it has been shown that in *Vibrio cholerae* deletion of Hfq affects pathogenesis due to disruption of the genes which are under transcriptional control of RpoS sigma factor (*13*). This suggests that Hfq influences RpoS translation, probably through association with an unidentified regulatory RNA in *V. cholerae*.

In order to identify orthologous DsrA RNA genes in other bacterial species with an *in silico* approach, it is necessary to develop a DsrA RNA secondary structure descriptor. Since there are two alternative models of its structure,

*Authors contributed equally to the work.
†To whom correspondence should be addressed. Tel: +48-61-8528 503 (Ext. 132), Fax: +48-61-8520 532, E-mail: Jan.Barciszewski@ibch.poznan.pl

we verified them experimentally. To get comprehensive results on DsrA RNA structure, we have applied the same methods as previously used by other authors (*5*, *7*) as well as novel RNA technologies, not used previously to study that RNA. Here, we present a new structural model for DsrA RNA. It is similar to the model I proposed initially by Sledjeski and Gottesman (*8*) and then by Majdalani *et al.* (*5*). It is a predicted rather than a confirmed model, and it differs significantly from the experimental model II proposed by Lease and Belfort (*7*). Our experimental data and bioinformatical calculations prove the new structure of the second hairpin and point to the conclusion that DsrA RNA has a dynamic nature. The data allowed us to propose new structural determinants of DsrA RNA. Moreover, since the second hairpin is crucial for DsrA function, our observations bring new insights into the mechanism of interaction of DsrA RNA.

MATERIALS AND METHODS

Preparation of DNA Plasmid Harboring DsrA RNA—A double-stranded 92 oligodeoxynucleotide was prepared by ligation of chemically synthesized short overlapping oligodeoxynucleotides of DsrA1—DsrA2 for one strand, and DsrA3—DsrA5 for the complementary one. The DNA fragments were inserted into the pT7/T3α-18 plasmid at the *Eco*RI and *Hin*dIII restriction sites. The *E. coli* NovaBlue (Novagen) bacterial strain was used as a host for the transformation. To confirm the correctness of ligation of the DNA fragments, the plasmid was isolated from transformants (QIAGEN Plasmid Midi Kit). The length of the ligation product was verified by PCR reaction and visualized on 2% agarose gel. The nucleotide sequence of the construct was confirmed by DNA sequencing using fmol DNA Sequencing System (Promega).

In Vitro *T7 RNA Transcription*—Plasmid (40 μg/ml) was cleaved with HindIII enzyme and the transcription was done with an Ambion Megashortscript T7 Transcription Kit. RNA was subsequently excised from a 10% denaturing polyacrylamide gel and eluted overnight in water at room temperature. RNA was precipitated with 2.5 volumes of 96% ethanol in the presence of 0.1 volume of 5 M ammonium acetate stop solution containing 100 mM EDTA (Ambion) and dissolved in RNase-free water (Ambion). The amount of RNA was calculated from the UV-absorbance measurements.

Labeling of DsrA RNA—The DsrA RNA (5 μg) was labeled at the 5′-end with [γ^{32}-P]ATP (ICN) and T4 polynucleotide kinase (5 U/μl) at 37°C for 45 min in the 10× reaction buffer containing 0.5 M Tris-HCl pH 7.6, 100 mM $MgCl_2$ and 100 mM 2-mercaptoethanol (Amersham Pharmacia). At the 3′-end the transcript was labeled with [^{32}P] pCp and T4 RNA ligase with a 10× reaction buffer containing 500 mM Tris-HCl pH 7.8, 100 mM $MgCl_2$, 50 mM DTT, 10 mM ATP (Promega) at 4°C for 14 h. The labeled DsrA RNA was purified on 10% polyacrylamide gel containing 7 M urea. The radioactive band was cut off. RNA was eluted with water overnight at room temperature and then, precipitated with 2.5 volumes 96% ethanol in the presence of 0.1 volume 5 M ammonium acetate with 100 mM EDTA (Ambion) and dissolved in RNase-free water (Ambion). The quantification of the labeled RNA was done by the scintillation counting.

Alkaline Hydrolysis—To generate a sequence ladder RNA, alkaline hydrolysis was performed at 95°C for 1.5 min in 10 μl of reaction mixture containing 50 mM NaOH, 1 mM EDTA and 4 μg of total RNA from *Lupinus luteus* as a carrier.

Nuclease Cleavages—The [^{32}P] labeled RNA (30,000 cpm) was treated with specific RNases. T1 RNase (Sigma) digestion was performed in a buffer containing 20 mM sodium citrate (pH 5.0), 7 M urea and 1 mM EDTA with 2.5 units of the enzyme, at 55°C for 20 min. RNase V1 digestion was done under native conditions, using (0.005 U/μl) RNase V1 (Ambion) in a buffer containing 50 mM Tris-HCl pH 7.2, 100 mM NaCl and 10 mM $MgCl_2$. The RNase S1 digestion in native conditions was done using (0.25 U/μl) RNase S1 (Promega) in the 10× reaction buffer [500 mM sodium acetate (pH 4.5), 280 mM NaCl and 45 mM $ZnSO_4$], supplied by the manufacturer (Promega). The reactions with V1 amd S1 were carried out for 10 minutes at 25°C. The footprinting results were analyzed with 20% PAGE.

RNase H Cleavage—Unlabeled RNA (1 pmol) and 30,000 cpm of labeled RNA were incubated with a 5-fold excess of oligodeoxynucleotide (L1: GAAATCTGAT, L2: AAGCAAGAAA, L3: TGAGGGGGTC or L4: AAAAAATTCGTT), and 0.4 U RNase H (Sigma) in a buffer containing 40 mM Tris-HCl pH 7.5, 4 mM $MgCl_2$, 0.1 mM DTT, 20 mM KCl in a total volume of 10 μl for 7.5 min at 37°C. Then 2 μl of 0.5 M EDTA was added to stop the reaction. The samples were denatured for 3 minutes at 65°C and analyzed on a 20% polyacrylamide gel with 7 M urea. The oligonucleotides complementary to different portions of putative regions of DsrA RNA were chemically synthesized (Institute of Biochemistry and Biophysics, Warsaw, Poland).

Cleavage with DNAzyme—Unlabeled (1 pmol) and 30,000 cpm of labeled DsrA RNA were incubated in the presence of a 5-, 10- or 15-fold excess of DNAzyme I and II in 50 mM Tris-HCl pH 7.5, respectively with DNAzyme I or II. Prior to the reaction, the target RNA and DNAzymes were denatured separately for 2 min at 85°C and cooled down to room temperature in a heating block. The reaction was initiated by the addition of $MgCl_2$ to a final concentration of 10 mM in a total volume of 10 μl. After incubation at 25°C for 30 min hydrolysis was stopped by the addition of 2 μl of 0.5 M EDTA and cooling on ice. The samples were analyzed on a 20% polyacrylamide gel with 7 M urea. The DNAzymes with sequences complementary to different portions of the putative regions were chemically synthesized (Institute of Biochemistry and Biophysic, Warsaw, Poland).

The Lead-Induced Hydrolysis—The [^{32}P]-labeled RNA supplemented with 2 μg of tRNA carrier was incubated in 50 mM Tris-HCl pH 7.5 with different concentrations of Pb^{2+} (1, 2.5 and 5 mM), at 25°C for 15 min. The hydrolysis products were analyzed by 20% PAGE.

Cleavage of RNA with Hydroxyl radicals—The cleavage reaction was carried out in 50 mM Tris-HCl, pH 7.5 containing 5 mM Fe(II), 2 mM EDTA, 5 μM DTT and with or without 10 mM $MgCl_2$ for 2 h at 25°C. The hydrolysis products were analyzed by 20% PAGE.

Hfq Protein Purification—Hfq was purified from *E. coli* harboring pET21b-plasmid with a His-Tag coding sequence. Cells were grown to 0.6 OD_{600} at 37°C, then

Hfq expression was induced with 1 mM IPTG. After 5 h the cells were harvested by centrifugation and resuspended in buffer A1-Ni-NTA (0.02 M imidazole, 0.1 M Tris pH 7.0, 0.05 M NaCl). The cells were ultrasonicated and cellular debris was removed by centrifugation. The supernatant was boiled for 10 min and centrifuged to remove the non-heat-stable proteins. The cleared supernatant was bound to Ni-NTA Agarose (Qiagen), incubated for 45 min at 25°C and centrifuged for 2 min at 8,000 rpm. The Ni-NTA was then washed three times with buffer A1-Ni- NTA. The Hfq protein was finally eluted with buffer B1-Ni-NTA containing different concentrations of imidazole (10, 50, 100 and 200 mM), and 0.1 M Tris-HCl, pH 7.0, 0.05 M NaCl. Hfq amount was determined by the Bradford method (*14*). The binding activity of the purified Hfq protein containing His-Tag was tested on 1% agarose gel (data not shown).

Cleavage Assay of DsrA RNA in the Complex with Hfq Protein—The [^{32}P] labeled DsrA RNA (30,000 cpm) and Hfq protein were incubated at 25°C for 20 min in 10 μl of reaction mixture in a buffer containing 10 mM Tris-HCl, pH 8.0, 50 mM NaCl, 50 mM KCl, 10 mM $MgCl_2$. The binding step was followed by cleavage with Pb^{2+} ions and hydroxyl radicals, as described above. All samples were analyzed by electrophoresis on a 20% PAGE.

Calculation of Structural Flexibility of DsrA RNA—To determine the structural stability of distinct regions of DrsA RNA, we used a statistical folding method (implemented in SFOLD: http://sfold.wadsworth.org) (*15*). The probability of existence of a nucleotide in a defined type of loop was used for further analysis. The probability of existence within the stem structure was calculated using the formula: $P_S = 1 - \Sigma P_L$ (P_S, probability of existence of a nucleotide within the stem structure; P_L, probability of existence of a nucleotide in a defined type of loop). The probability of secondary structure flexibility was calculated as follows: $P_F = 1 - P_{max}$ (P_F, probability of structural flexibility; P_{max}, maximum probability of existence of a nucleotide within the stem or a defined type of loop).

RESULTS

Computational Analysis—The very first step of our studies was computational analysis of the DsrA RNA nucleotide sequence. The secondary structure prediction using MFOLD (*16*) revealed a minimum free energy structure which was the same as that described for the model I of DsrA RNA (*5*). Other suboptimal structures were also calculated, but none of them was similar to that proposed by Lease and Belfort (*7*). Surprisingly, the calculations performed for different portions (hairpins) of the DsrA RNA structure reveal that hairpin 2 of model II has positive free energy (Table 1), which indicated that formation of such structure is not thermodynamically favored. To find energetically favorable conformations of the central region of DsrA RNA, we used the nucleotide sequence string between hairpins 1 and 3. Only short (4 nt long) stems, not present in any of the known models, were predicted (data not shown).

To verify if the middle region of DsrA RNA is highly structured, we carried out a statistical folding (SFOLD) analysis (*15*). Our calculations of DsrA RNA revealed that hairpins 1 and 3 are extremely stable (Fig. 1). There are no other possibilities of alternative base pairings for these regions and a conformation once acquired not can be disrupted. Conversely, the central region of DsrA RNA revealed relatively high diversity of possible base pairings and stem locations.

RNases Footprintings—RNases footprintings were used to propose model II (*7*). We have also carried out a experiments with the same nucleases in order to verify the

Table 1. **Free energy (kcal/mol) of overall structure and hairpin 2 of DsrA RNA models calculated using MFOLD (*16*).**

Model	Overall	Hairpin 2	Reference
Model I	–31.8	–5.2	(*5*)
Model II	–23.9	2.6	(*7*)
Model III	–28.4	–2.8	(This paper)

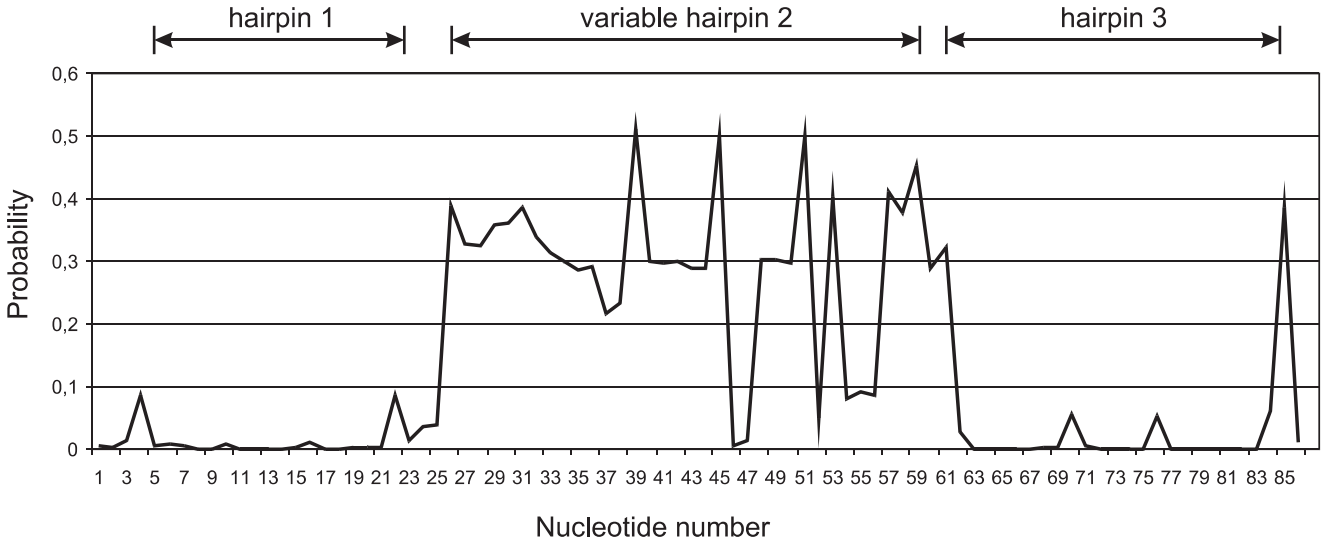

Fig. 1. **Structural flexibility of DsrA RNA.** Probabilities of existence of a nucleotide in alternative structures have been calculated. The central stem-loop region reveals relative high flexibility in comparison to the rest of the particle.

previous data. The RNase T1, V1 and S1 footprintings on DsrA RNA labeled at the 5′ and 3′ ends essentially confirm the structure of stem-loops 1 and 3, which in fact, are the same for both models (Fig. 2). However, in contrast to model II, we observed strong hydrolysis by RNase V1 that is specific for double-stranded RNA at positions 28–32 of hairpin 2. This observation is consistent with the structure of the second stem-loop proposed in model I. It clearly shows that these nucleotides are involved in stem formation rather than being single-stranded, as is proposed in model II (Fig. 2, A and C). We propose location of this region in a stem of the hairpin 2 (Fig. 2C, III).

Our nuclease S1 results did not show cleavage at positions 29–34 (Fig. 2, A and C). This clearly indicates that the single-stranded region between hairpins 1 and 2 that was proposed earlier in model II does not exist. Although these data seem to be consistent with model I, we observed additional S1 cleavage sites at nucleotides 38 and 39 (Fig. 2C). This result suggested different localization of the loop region in hairpin 2. Based on S1 hydrolysis at positions 36 and 37 and V1 cleavage at positions 28–32, 34 and 47, we proposed the new structure of hairpin 2 (Fig. 2C, III).

RNase H Hydrolysis—To confirm our DsrA RNA secondary structure model, we used RNase H to digest DsrA RNA in the presence of oligodeoxynucleotides complementary to

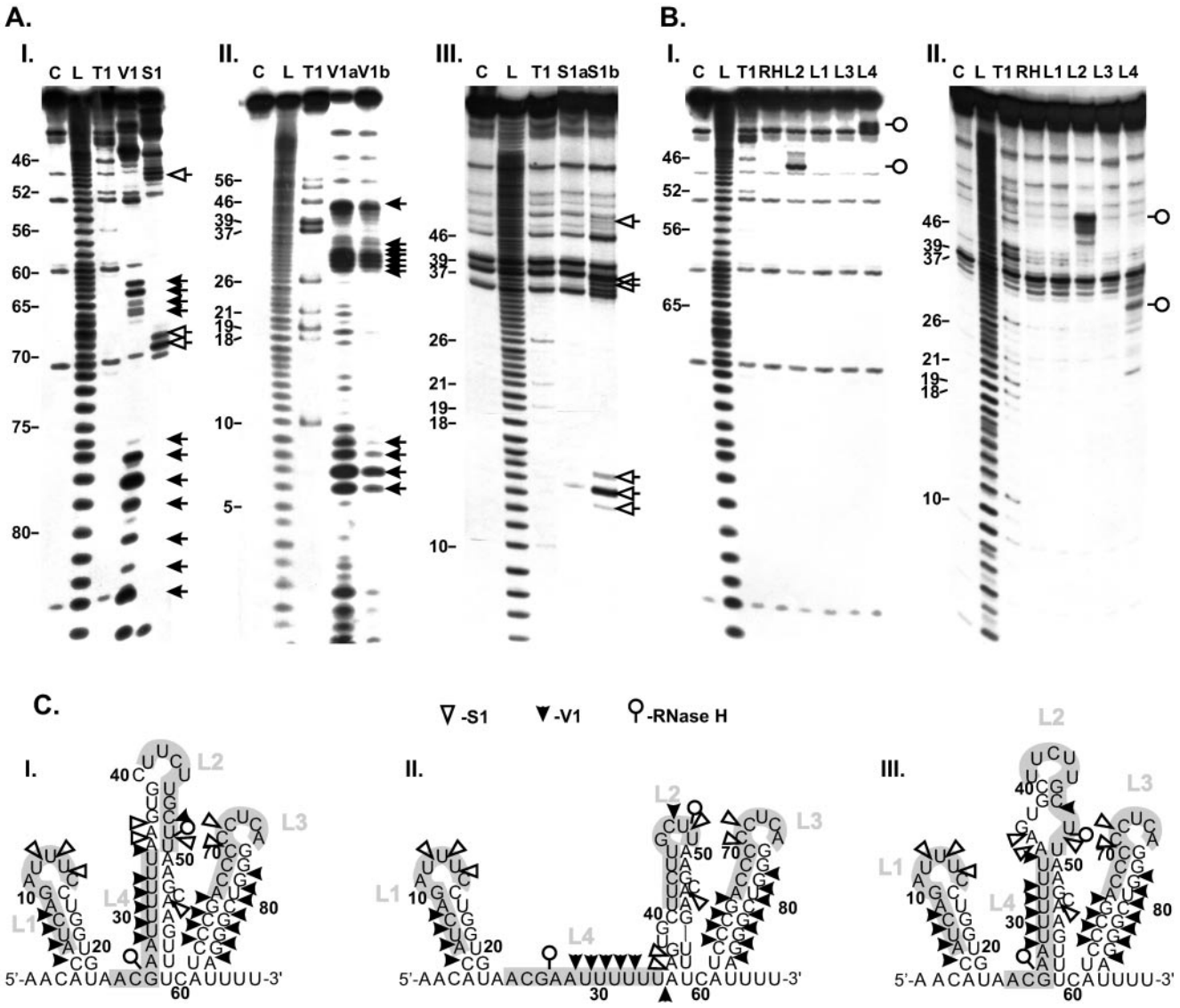

Fig. 2. **Autoradiogram of 20% polyacrylamide gel electrophoresis of partial hydrolysate.** (A) 3′ [^{32}P] (I), and 5′ [^{32}P] (II and III)–labeled DsrA RNA with different amounts of V1and S1 RNases. Lanes: C, control RNA; L, alkaline hydrolysis ladder; T1, limited hydrolysis with RNase T1; V1(I), V1a and V1b(II), partial hydrolysis with 0.003, 0.01 and 0.005 U of V1 RNase, respectively; S1(I), S1a and S1b(III), partial hydrolysis with 0.25, 0.125 and 0.25 U of S1 RNase, respectively. (B) 3′ [^{32}P]-(I), and 5′ [^{32}P]-(II)–labeled DsrA RNA with RNase H in presence of different oligodeoxynucleotides. Lanes: C, control RNA; L, alkaline hydrolysis ladder; T1, limited hydrolysis with RNase T1; RH, DsrA RNA with RNase H in the absence of oligonucleotide; L1-L4, hydrolysis of DsrA RNA with 0.4 U of RNaseH and oligonucleotide L1, L2, L3 and L4, respectively. (C) The secondary structure models of DsrA RNA: I (*5*), II (*7*) and III (this paper). Fragments of DsrA RNA complementary to oligonudeoxynucleotides L1–L4 are shadowed. The enzymatic cleavage patterns are consistent only with model III.

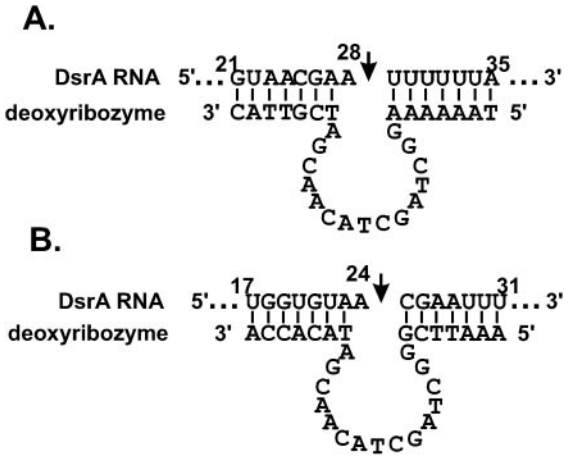

Fig. 3. **The secondary structure of DNAzymes A and B designed to cleave DsrA RNA at *a priori* predicted sites (marked with arrows).**

the loops of hairpins 1, 2 and 3 (L1–L3) and, finally, to the single-stranded region (nucleotides 24–34) proposed in model II (L4). We observed two main cleavage sites at nucleotides 26 and 48 (Fig. 2, B and C). Since RNase H can hydrolyze only RNA-DNA heteroduplex (*17*, *18*), the observed cleavage pattern confirms that targeted region is single-stranded. Hydrolysis at nucleotide 26 confirms the lack of long single-stranded region between hairpins 1 and 2 as in model II. Instead the cleavage site at the 5′ end corresponds to the middle part of the antisense oligonucleotide. This suggests a short stretch of the oligonucleotide able to hybridize because the stem begins with nucleotide 26, which creates a new 5′ end of the duplex. The cleavage at that position supports our model (Fig. 2, B and C). Interestingly, we also noticed additional RNase H hydrolysis products at positions 45–47, with different length than the main product.

Cleavage with DNAzymes—To confirm the lack of the long single-stranded region between hairpins 1 and 2 proposed in model II, we designed two DNAzymes (Fig. 3) (*19*). DNAzymes are RNA-cleaving agents with conserved catalytic domains flanked by variable binding domains (*20*). They target single-stranded DNA or RNA in the presence of divalent cations (*21–24*). We used magnesium-dependent deoxyribozymes. If the regions G_{21}–A_{35} and U_{17}–U_{31} interact with DNAzyme I and II, respectively, one may expect cleavage at A_{28} and A_{24}, respectively (Fig. 3). However, such hydrolysis was not observed. This supports our finding that the previously proposed single-stranded region (23–34nt) is, in fact, double-stranded.

Interactions of DsrA RNA with Hfq Protein—To identify the nucleotides involved in the interactions with Hfq protein, we designed experiments with hydroxyl radical and Pb^{2+} cleavage.

Hydrolysis with Hydroxyl Radicals—To get a better insight into the structural dynamics of DsrA RNA in the interaction with Hfq protein, we used a Fe(II)-EDTA solvent-based reagent (*25*). In the absence of Mg^{2+} ions, DsrA RNA was more susceptible to hydrolysis than in the presence of Mg^{2+}. This is consistent with previous results showing that Mg^{2+} ions stabilize the secondary structure of RNA (Fig. 4A) (*26*, *27*). The hydrolysis pattern of DsrA RNA in the presence and absence of Hfq protein was different. The data show that the regions of hairpin 2 spanning nucleotides 51–52, 55–58, 61–64 and 66–70 are strongly protected by the protein from hydrolysis by hydroxyl radicals (Fig. 4, A and C).

Lead-Induced Hydrolysis—Lead induces hydrolysis in regions 42–49 and 57–60 of DsrA RNA. In the presence of Hfq protein, we observed strong protection against cleavage at nucleotides 43–52, 57–59 and 69–71 (Fig. 4B). Involvement of these nucleotides in protein-RNA interaction is consistent with hydroxyl radical cleavage pattern. The nucleotides 43–50 and 71 were protected against cleavage by lead, but not against hydroxyl radicals. Moreover, in the presence of Hfq, we observed additional cleavage sites around nucleotides 10 and 30. Since lead-induced cleavage is structure-dependent, these differences identify structural changes in DsrA RNA affected by the Hfq binding.

Nucleotides 60–63 and 65–68 were cleaved by hydroxyl radicals, but not by lead neither in presence nor absence of Hfq protein. This may be an effect of structural inaccessibility of those nucleotides. It means that those regions form the core of DsrA RNA tertiary structure.

DISCUSSION

Deep understanding of non-protein-coding RNAs is still hampered by the lack of efficient methods for their identification. The best solution would be a descriptor of preserved domains, characteristic and well conserved through evolution. Two different models of DsrA RNA secondary structure have been already proposed (*5*, *7*). The first one (model I) is based on thermodynamic calculations and mutation analysis (*5*). It consists of three stem-loops and one short single-stranded region between hairpins 1 and 2. Model II, currently believed to be the correct one, is supported by specific nuclease cleavage experiments (*7*). It has similar stem-loops 1 and 3 to those in the model I, but a different structure for hairpin 2.

We began our study on DsrA RNA structure with computational analysis of its sequence. The statistical folding experiment reveals a relatively high structural flexibility of its central region (Fig. 1). This feature of DsrA RNA raises a question about the energy and structural stability of the second hairpin loop proposed in models I and II. Thus, we calculated the free energy for both versions of hairpin 2 (Table 1). The results clearly show that the conformation of this region proposed in model II is very unlikely due the positive free energy. For the energy calculations only secondary structure energy values were used and therefore the possibility that this hairpin loop is stabilized by strong tertiary interactions or external factors (*e.g.* proteins) cannot be excluded. Thus, we decided to use a verification method independent from energy calculations. It is based on covariation of mutations in DsrA RNA sequences from different organisms. Currently, there are five DsrA RNA sequences known: *Escherichia coli*, *Salmonella typhimurium*, *Salmonella enterica*, *Shigella sonnei* and *Shigella flexneri*. The nucleotide sequences of DsrA RNA from *E. col*i and two species of *Shigella* are 99% identical, as are those from the

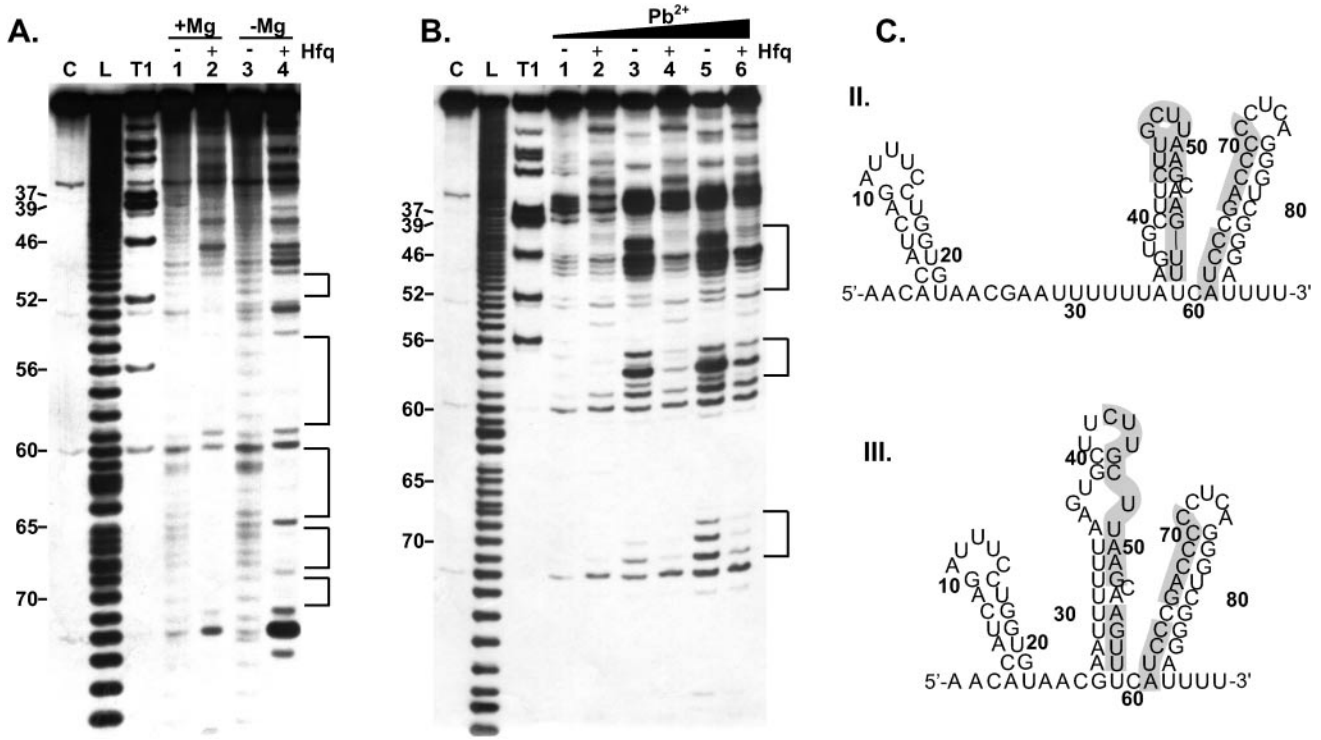

Fig. 4. **Autoradiogram of a 20% polyacrylamide gel analysis of the hydrolysis products of 3′ [^{32}P] labeled DsrA RNA with hydroxyl radical (A) and Pb^{2+} (B) ions in the presence and absence of Hfq protein.** Lines: C, untreated control RNA; L, alkaline hydrolysis ladder; T1, limited hydrolysis with RNase T1; A) 1-2, hydrolysis with hydroxyl radical in the presenceof magnesium ions, in the absence (lane 1) and in the presence (lane 2) of Hfq protein; 3-4, hydrolysis with hydroxyl radicals in the absence of magnesium ions, in the absence (lane 3) and in the presence (lane 4) of Hfq protein; B) 1-2, hydrolysis with Pb^{2+} ions (1 mM) in the absence (lane 1) and in the presence of Hfq protein (lane 2); 3-4, hydrolysis with Pb^{2+} ions (2.5 mM) in the absence (lane 3) and in the presence (lane 4) of Hfq protein; 5-6, hydrolysis with Pb^{2+} ions (5 mM) in the absence (lane 5) and in the presence (lane 6) of Hfq protein. C) Regions protected from hydroxyl radicals and lead-induced cleavage by Hfq binding marked on models II (*7*) and III (this paper) of DsrA RNA secondary structure. No protection was observed on poly-U tract in positions 31–36, proposed to be the main Hfq binding site on DsrA RNA.

two *Salmonella* species. This resulted in only two non-redundant sequences. Because of this small dataset, we decided to align the DsrA RNA sequences manually to both models proposed previously and obtained in our further experimental studies. We observed no compensatory base changes favoring any of the models (data not shown).

To verify the DsrA RNA structure model II proposed by Lease and Belfort (*7*), we performed a new set of experimental studies. In addition to the previously used tools, we applied novel methods, not used before for the analysis of DsrA RNA secondary structure. Its primary aim was to prove the existence of the long single-stranded region between hairpins 1 and 2 proposed earlier in model II, which is thought to be the main Hfq binding site.

Generally, our results clearly suggest that this region between hairpins 1 and 2 is double-stranded. The strongest evidence which supports such a model is the set of RNase V1 cleavages observed at nucleotides 28–32. In the previous work (*7*), this part of the molecule was cleaved by RNase S1. This was not a case in our studies. Interestingly, hydrolysis by RNase V1 at position 27 was also observed in the previous work (*7*), although model II does not accommodate this site in a double-stranded part. Our model fully accommodates this cleavage. The single-stranded region between hairpins 1 and 2 was also excluded by the lack of cleavage with the designed DNAzymes (this work). Also, the RNase H hydrolysis experiments did not reveal the ability of this region to bind oligodeoxynucleotide and strongly confirm that DsrA RNA has a dynamic structure. Additional cleavages at nucleotides 45–47 show that there are several structural isoforms possible with different abilities to bind oligonucleotides. Therefore, hybridization of oligonucleotides complementary to the central region of DsrA RNA, followed by RNase H cleavage sites, together with lack of hydrolysis in case of the oligonucleotides complementary to hairpins 1 and 3 constitute the best evidence for the dynamic character of hairpin 2 and the high stability of the hairpins 1 and 3, which are inaccessible for hybridization.

The reason for the differences in V1 and S1 RNases cleavage patterns between our data and Lease and Belfort's (*7*) results is not clear. No details are available of the conditions used in experiments performed by Lease and Belfort (*7*). However, we suppose that the structural differences observed are effects of magnesium concentration. Because of the well-documented impact of magnesium ions on RNA structure (*28*), we carefully controlled the experimental conditions. We removed the magnesium ions used for the DsrA RNA preparation by adding EDTA in each precipitation step. After the very last step of purification, DsrA RNA was dissolved in pure RNase-free water, instead of

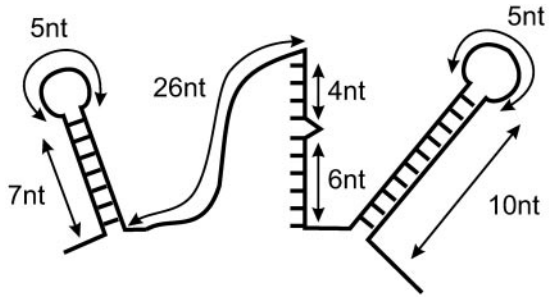

Fig. 5. **The secondary structure determinants of DsrA RNA.** The model consists of highly defined stems 1 and 3, and a sequence located upstream from stem 3, which takes part in interaction with Hfq protein and should be double-stranded.

DEPC traeted water, as in Lease and Belfort's studies (*9*). This approach provides an RNA sample containing only trace amounts of magnesium ions.

Structural differences observed in our studies can be explained also by variations in the primary sequence of the RNA transcript. DsrA RNA that we worked with shows exactly the same sequence as reported in GeneBank database, whereas the transcript used by Lease and Belfort had two additional guanosines at the 5′ end and lacked one uridine at the 3′ end. One should also notice that differences between the models II (*7*) and III (this paper) could result from higher concentration of RNase V1 used by Lease and Belfort and elution of RNA from the gel at 60°C which might induce degradation of the material.

The absence of a single-stranded region between hairpins 1 and 2 demonstrated in our studies has a big impact on our understanding of DsrA RNA action. It has been shown that DsrA RNA has several Hfq binding sites (*9*). At low Hfq concentration, one of the sites seems to bind the Hfq necessary for interaction with target mRNAs (*9*). At high Hfq concentration additional Hfq molecules are bound under, which causes DsrA arrest and stops its interaction with RpoS mRNA.

We did not observe any protection by Hfq against hydroxyl or lead-induced hydrolysis in the region between hairpins 1 and 2 as has been suggested by model II studies. Instead, we clearly identified regions in stems 2 and 3, that are consistent with previous reports on the importance of these sites in Hfq binding (*10*). However, the mutations introduced in the DsrA RNA poly-U tract resulted in the loss of Hfq binding and loss of DsrA RNA function (*10*). Since the mutations occur in the stem region of the second hairpin loop, we propose from our model that the observed effect was not due to mutation of the Hfq binding sequence, but rather because of disruption of key structural features necessary for Hfq binding. Our results indicate that the poly-U tract sequence is not involved in Hfq binding, but this aspect still needs more detailed studies.

In summary, our results deny the existence and importance of a long single-stranded region between hairpins 1 and 2. Thus also allow us to propose a secondary structure descriptor of DsrA RNA, which does not include this region as a DsrA RNA determinant (Fig. 5). The new model of DsrA RNA secondary structure clearly indicates that the mechanism of Hfq-dependent regulation by DsrA RNA proposed previously needs to be revised.

We would like to thank Gisela Storz for her kind gift of pET21b-plasmid. This work was supported with a grant from the Polish Ministry of Science and Education no. 2 PO4A 046 29. MZ doctoral scholarship was funded by the President of the Polish Academy of Sciences.

REFERENCES

1. Venter, J.C., Adams, M.D., Myers, E.W., Li, P.W., Mural, R.J., Sutton, G.G., Smith, H.O., Yandell, M., Evans, C.A., Holt, R.A., *et al.* (2001) The sequence of the human genome. *Science* **291**, 1304–1351
2. Rodriguez, A., Griffiths-Jones, S., Ashurst, J.L., and Bradley, A. (2004) Identification of mammalian microRNA host genes and transcription units. *Genome Res.* **14**, 1902–1910
3. Yano, Y., Saito, R., Yoshida, N., Yoshiki, A., Wynshaw-Boris, A., Tomita, M., and Hirotsune, S. (2004) A new role for expressed pseudogenes as ncRNA: regulation of mRNA stability of its homologous coding gene. *J. Mol. Med.* **82**, 414–422
4. Gottesman, S. (2004) The small RNA regulators of *Escherichia coli*: roles and mechanisms. *Annu. Rev. Microbiol.* **58**, 303–328
5. Majdalani, N., Cunning, C., Sledjeski, D., Elliott, T., and Gottesman, S. (1998) DsrA RNA regulates translation of RpoS message by an anti-antisense mechanism, independent of its action as an antisilencer of transcription. *Proc. Natl. Acad. Sci. USA* **95**, 12462–12467
6. Kolb, F.A., Engdahl, H.M., Slagter-Jager, J.G., Ehresmann, B., Ehresmann, C., Westhof, E., Wagner, E.G., and Romby, P. (2000) Progression of a loop-loop complex to a four-way junction is crucial for the activity of a regulatory antisense RNA. *EMBO J.* **19**, 5905–5915
7. Lease, R.A. and Belfort, M. (2000) A trans-acting RNA as a control switch in *Escherichia coli*: DsrA modulates function by forming alternative structures. *Proc. Natl. Acad. Sci. USA* **97**, 9919–9924
8. Sledjeski, D. and Gottesman, S. (1995) A small RNA acts as an antisilencer of the H-NS silenced rcsA gene of *Escherichia coli*. *Proc. Natl. Acad. Sci. USA* **92**, 2003–2007
9. Lease, R.A. and Woodson, S.A. (2004) Cycling of the Sm-like protein Hfq on the DsrA small regulatory RNA. *J. Mol. Biol.* **344**, 1211–1223
10. Brescia, C.C., Mikulecky, P.J., Feig, A.L., and Sledjeski, D.D. (2003) Identification of the Hfq-binding site on DsrA RNA: Hfq binds without altering DsrA secondary structure. *RNA* **9**, 33–43
11. Sledjeski, D.D., Whitman, C., and Zhang, A. (2001) Hfq is necessary for regulation by the untranslated RNA DsrA. *J. Bacteriol.* **183**, 1997–2005
12. Mikulecky, P.J., Kaw, M.K., Brescia, C.C., Takach, J.C., Sledjeski, D.D., and Feig, A.L. (2004) *Escherichia coli* Hfq has distinct interaction surfaces for DsrA, rpoS and poly (A) RNAs. *Nat. Struct. Mol. Biol.* **11**, 1206–1214
13. Ding, Y., Davis, B.M., and Waldor, M.K. (2004) Hfq is essential for Vibrio cholerae virulence and downregulates sigma expression. *Mol. Microbiol.* **53**, 345–354
14. Bradford, M.M. (1976) A rapid and sensitive method for the quantitation of microgram quantities of protein utilizing the principle of protein-dye binding. *Anal. Biochem.* **72**, 248–254
15. Ding, Y., Chan, C.Y., and Lawrence, C.E. (2004) Sfold web server for statistical folding and rational design of nucleic acids. *Nucleic Acids Res.* **32**, W135–141
16. Zuker, M. (2003) Mfold web server for nucleic acid folding and hybridization prediction. *Nucleic Acids Res.* **31**, 3406–3415
17. Crooke, S.T., Lemonidis, K.M., Neilson, L., Griffey, R., Lesnik, E.A., and Monia, B.P. (1995) Kinetic characteristics of *Escherichia coli* RNase H1: cleavage of various antisense oligonucleotide-RNA duplexes. *Biochem. J.* **312** (Pt 2), 599–608

18. Wu, H., Lima, W.F., and Crooke, S.T. (1999) Properties of cloned and expressed human RNase H1. *J. Biol. Chem.* **274**, 28270–28278
19. Sun, L.Q., Cairns, M.J., Saravolac, E.G., Baker, A., and Gerlach, W.L. (2000) Catalytic nucleic acids: from lab to applications. *Pharmacol. Rev.* **52**, 325–347
20. Santoro, S.W. and Joyce, G.F. (1997) A general purpose RNA-cleaving DNA enzyme. *Proc. Natl. Acad. Sci. USA* **94**, 4262–4266
21. Cuenoud, B. and Szostak, J.W. (1995) A DNA metalloenzyme with DNA ligase activity. *Nature* **375**, 611–614
22. Breaker, R.R. and Joyce, G.F. (1994) A DNA enzyme that cleaves RNA. *Chem. Biol.* **1**, 223–229
23. Breaker, R.R. and Joyce, G.F. (1995) A DNA enzyme with Mg^{2+}-dependent RNA phosphoesterase activity. *Chem. Biol.* **2**, 655–660
24. Carmi, N., Shultz, L.A., and Breaker, R.R. (1996) In vitro selection of self-cleaving DNAs. *Chem. Biol.* **3**, 1039–1046
25. Barciszewska, M.Z., Erdmann, V.A., and Barciszewski, J. (1994) The dynamic conformation of plant cytoplasmic 5S rRNAs. *Phytochemistry* **37**, 113–117
26. Serebrov, V., Vassilenko, K., Kholod, N., Gross, H.J., and Kisselev, L. (1998) Mg^{2+} binding and structural stability of mature and in vitro synthesized unmodified *Escherichia coli* tRNAPhe. *Nucleic Acids Res.* **26**, 2723–2728
27. Brion, P., Michel, F., Schroeder, R., and Westhof, E. (1999) Analysis of the cooperative thermal unfolding of the td intron of bacteriophage T4. *Nucleic Acids Res.* **27**, 2494–2502
28. Petyuk, V.A., Zenkova, M.A., Giege, R., and Vlassov, V.V. (1999) Hybridization of antisense oligonucleotides with the 3′ part of tRNA(Phe). *FEBS Lett.* **444**, 217–221